Bespoken Nanoceria: An Effective Treatment in Experimental Hepatocellular Carcinoma

Guillermo Fernández-Varo [ID] ,[1,2] Meritxell Perramón [ID] ,[1] Silvia Carvajal,[1] Denise Oró,[1] Eudald Casals,[3] Loreto Boix,[4] Laura Oller,[1] Laura Macías-Muñoz,[1] Santi Marfà,[1] Gregori Casals,[1,5] Manuel Morales-Ruiz,[1,2,5] Pedro Casado [ID] ,[6] Pedro R. Cutillas,[6] Jordi Bruix,[4] Miquel Navasa,[7] Josep Fuster,[7] Juan Carlos Garcia-Valdecasas,[7] Mihai C. Pavel,[7] Víctor Puntes,[8-10] and Wladimiro Jiménez [ID] [1,2]

BACKGROUND AND AIMS: Despite the availability of new-generation drugs, hepatocellular carcinoma (HCC) is still the third most frequent cause of cancer-related deaths worldwide. Cerium oxide nanoparticles (CeO₂NPs) have emerged as an antioxidant agent in experimental liver disease because of their antioxidant, anti-inflammatory, and antisteatotic properties. In the present study, we aimed to elucidate the potential of CeO_2NPs as therapeutic agents in HCC.

APPROACH AND RESULTS: HCC was induced in 110 Wistar rats by intraperitoneal administration of diethylnitrosamine for 16 weeks. Animals were treated with vehicle or CeO_2NPs at weeks 16 and 17. At the eighteenth week, nanoceria biodistribution was assessed by mass spectrometry (MS). The effect of CeO_2NPs on tumor progression and animal survival was investigated. Hepatic tissue MS-based phosphoproteomics as well as analysis of principal lipid components were performed. The intracellular uptake of CeO_2NPs by human *ex vivo* perfused livers and human hepatocytes was analyzed. Nanoceria was mainly accumulated in the liver, where it reduced macrophage infiltration and inflammatory gene expression. Nanoceria treatment increased liver apoptotic activity, while proliferation was attenuated. Phosphoproteomic analysis revealed that CeO_2NPs affected the phosphorylation of proteins mainly related to cell adhesion and RNA splicing. CeO_2NPs decreased phosphatidylcholine-derived arachidonic acid and reverted the HCC-induced increase of linoleic acid in several lipid components. Furthermore, CeO_2NPs reduced serum alpha-protein levels and improved the survival of HCC rats. Nanoceria uptake by *ex vivo* perfused human livers and *in vitro* human hepatocytes was also demonstrated.

CONCLUSIONS: These data indicate that CeO_2NPs partially revert the cellular mechanisms involved in tumor progression and significantly increase survival in HCC rats, suggesting that they could be effective in patients with HCC. (HEPATOLOGY 2020;72:1267-1282).

Hepatocellular carcinoma (HCC) is the third leading cause of death by cancer worldwide.[1] HCC commonly arises in patients with underlying chronic liver disease and is considered a typical inflammation-associated tumor.[2] The appearance of cirrhosis greatly favors the onset of HCC through mechanisms not yet well known that began to be elucidated in recent years.[3] In the last decade, complex

genetic alterations, epigenetic chromosomal aberrations, and cellular signaling pathways triggering tumor development, progression, and metastasis have been characterized.[4] The current systemic treatments of HCC are based on molecularly targeted therapies. Sorafenib, a multikinase inhibitor, was the first compound for first-line treatment of patients with advanced-stage HCC.[5] However, clinical trials have found only modest improvement in overall survival,[6] and the emergence of resistance episodes reveals the need to develop effective therapies for HCC.[7] Although the available drugs improve clinical outcomes, the median overall survival continues to be approximately 1 year.[8,9]

Of particular importance is the role of reactive oxygen species (ROS) in the onset and progression of HCC.[10] Mechanistic studies show that ROS induce alterations in DNA and modify key cellular processes such as cell proliferation and apoptosis.[11] Thus, it has been hypothesized that HCC develops because chronic oxidative stress exerts a selective pressure that favors the outgrowth of cells from progenitor clones that are more resistant to oxidative damage.[12]

Antioxidant agents have demonstrated their efficacy in chronic liver diseases equilibrating hepatic ROS metabolism, thereby improving liver functionality.[13]

Recently, cerium oxide nanoparticles (CeO_2NPs) have emerged as an antioxidant and anti-inflammatory agent. Superoxide dismutase activity[14] (conversion of superoxide anion into hydrogen peroxide and finally oxygen), catalase activity[15,16] (hydrogen peroxide into oxygen and water), and peroxidase activity[17] (hydrogen peroxide into hydroxyl radicals), among others, have been attributed to CeO_2NPs. Consequently, the wide spectrum of antioxidant enzyme-mimetic activities of CeO_2NPs has been explored in the treatment of many diseases related to the overproduction of ROS. Thus, the ability of CeO_2NPs to modulate oxidative stress in diseases ranging from retinal degeneration,[18] neurodegenerative diseases,[19] diabetes,[20] ischemia,[21] cardiopathies,[22] gastrointestinal inflammation,[23] and especially cancer has been described.[24-27] As well, the therapeutic possibilities of CeO_2NPs have been shown in the case of experimental liver disease.[28-32]

ARTICLE INFORMATION:

From the [1]Service of Biochemistry and Molecular Genetics, Hospital Clinic Universitari, Centro de Investigación Biomédica en Red de Enfermedades Hepáticas y Digestivas (CIBERehd), Institut d'Investigacions Biomèdiques August Pi i Sunyer (IDIBAPS), Barcelona, Spain; [2]Departament of Biomedicine, University of Barcelona, Barcelona, Spain; [3]School of Biotechnology and Health Sciences, Wuyi University, Jiangmen, China; [4]Barcelona-Clinic Liver Cancer Group, Liver Unit, Hospital Clinic de Barcelona, CIBERehd, IDIBAPS, University of Barcelona, Barcelona, Spain; [5]Working Group for the Biochemical Assessment of Hepatic Disease-SEQC[ML], Barcelona, Spain; [6]Centre for Haemato-Oncology, Barts Cancer Institute, Queen Mary University of London, London, UK; [7]Liver Surgery and Transplant Unit, Digestive and Metabolic Diseases Institute, Hospital Clínic of Barcelona, CIBERehd, IDIBAPS, University of Barcelona, Barcelona, Spain; [8]Institut Català de Recerca i Estudis Avançats (ICREA), Barcelona, Spain; [9]Institut Català de Nanociència i Nanotecnologia (ICN2), Bellaterra, Spain; [10]Vall d'Hebron Institute of Research (VHIR), Barcelona, Spain.

ADDRESS CORRESPONDENCE AND REPRINT REQUESTS TO:

Wladimiro Jiménez, Ph.D.
Servicio de Bioquímica y Genética Molecular
Hospital Clinic Universitario
Villarroel 170
Barcelona 08036, Spain
E-mail: wjimenez@clinic.cat
Tel.: +34 93 2275400 ext. 3091

or

Victor Puntes, Ph.D.
Institut Català de Nanociència i Nanotecnología, Campus UAB
Barcelona 08193, Spain
E-mail: victor.puntes@icn2.cat
Tel.: +34 93 7374622

We considered the potential therapeutic value of CeO_2NPs in an experimental model of HCC in rats by chronic administration of diethylnitrosamine (DEN). We assessed the impact of CeO_2NPs on tumor progression and survival, the accumulation in isolated human liver, and their intracellular adsorption by human liver-derived cancer cells.

Material and Methods

SYNTHESIS AND CHARACTERIZATION OF RAT SERUM ALBUMIN STABILIZED CeO_2NPs

CeO_2NPs of 4-5 nm were synthesized by the chemical precipitation of cerium (III) nitrate hexahydrate (Sigma-Aldrich, St. Louis, MO) in a basic aqueous solution.[14,15,17,28] Cerium (III), 10 mM, was dissolved in 100 mL of Milli-Q water at room temperature. To this, 3 mL of tetramethylammonium hydroxide (TMAOH) solution (1 M) was added slowly at room temperature under vigorous stirring (final concentration of 10 mM), and the mixture was allowed to age under mild stirring overnight. During the first minutes, the solution is colorless, and then it turns progressively brownish. Afterward, nanoparticles (NPs) were purified by centrifugation ($10,000g$, 10 minutes, at room temperature), and the resultant pellet was resuspended in 100 mL aqueous solution of 1 mM TMAOH. The xylenol orange test and inductively coupled plasma–mass spectrometry (ICP-MS) indicated a full conversion of Ce to CeO_2NPs. Thus, the final CeO_2 concentration for this synthesis was determined to be 1.72 mg/mL ($6.7 \cdot 10^{15}$ NPs/mL) and then diluted to the 1 mg/mL employed solution. Further details on CeO_2NPs synthesis and characterization can be found in the Supporting Information.

CeO_2NPs ADMINISTRATION

CeO_2NPs or vehicle were dispersed in saline solution and intravenously given as a bolus (500 µL) through the tail vein. CeO_2NPs (0.1 mg/kg body weight) or vehicle (saline solution containing TMAOH ammonium salts 0.8 mM) were injected twice a week for 2 consecutive weeks starting at the sixteenth week after beginning DEN administration.

HCC INDUCTION IN RATS

Experimental studies were performed in 118 male Wistar rats weighing 200 g (Charles-River, Saint Aubin les Elseuf, France). HCC was chemically induced in 110 rats by an intraperitoneal administration of DEN (50 mg/kg body weight; Sigma-Aldrich) once a week for 16 weeks, and eight healthy rats were included as a control group.

ACCUMULATION OF Ce IN ISOLATED HUMAN LIVERS

To assess whether the human liver parallels the kinetic adsorption pattern shown by CeO_2NPs in the rat liver, human livers from three donors, designated subjects H1, H2, and H3, were used in the present study. Livers were procured in the Hospital Clinic (Barcelona, Spain), rejected for transplantation, and approved for research.

CeO_2NPs ADSORPTION BY HUMAN HEPATOCYTE CANCER CELLS

To investigate whether human hepatocytes are able to intracellularly take up CeO_2NPs, subsequent studies were performed in HepG2 cells, a human cell line derived from a liver HCC (ATCC, Manassas, VA).

ETHICAL APPROVAL

The study was approved and performed according to the criteria of the Investigation and Ethics Committee of the Hospital Clínic Universitari (Barcelona, Spain). Animals received humane care according to the criteria outlined in the "Guide for the Care and Use of Laboratory Animals". The study of the human livers was conducted in the Hospital Clínic de Barcelona, which is part of the European Union–funded Consortium for Organ Preservation in Europe (http://www.ope-eu.com).

For further information, please refer to the Supporting Information.

Results

CHARACTERIZATION OF CeO_2NPs

A description of the characterization of the CeO_2NPs used in this study has been published.[32] High-resolution transmission electron microscopic

(TEM) analysis indicated that the NPs had a spherical morphology and were predominantly within the size range of 4-20 nm. The X-ray diffraction pattern showed pure CeO$_2$NPs with the typical peak broadening characteristic of nanosized particles. Initially, the employed NPs are positively charged, and the colloidal stability is mediated by electrostatic repulsion (zeta potential +43.0 ± 1.3 mV, conductivity 0.303 ± 0.006 mS/cm, and pH 4.3). Albumin conjugation in the surface of the CeO$_2$NPs has been characterized by the increase in dynamic light scattering (from 5 to 20 nm) and decrease in zeta potential (from +42.8 to –10 mV, which is the average zeta potential value of proteins in serum) (Supporting Fig. S1). Indeed, the solubility of CeO$_2$NPs in physiological media is challenging, and a strong tendency to aggregate and sediment impedes their medical use even more, modifying their protective effects toward the proinflammatory (https://www.frontiersin.org/articles/10.3389/fimmu.2017.00970/full). To evaluate the electronic structure of the CeO$_2$NPs and the influence on Ce valence state due to the presence of rat serum albumin, we performed X-ray photoelectron spectroscopy measurements. Ce three-dimensional spectra of all samples are shown in Supporting Fig. S2, where it can be clearly observed that the Ce^{3+}/Ce^{4+} ratio is not affected by the presence of bovine serum albumin in the CeO$_2$NPs surface.

THE RAT MODEL OF DEN-INDUCED LIVER INJURY EXHIBITS CHARACTERISTICS OF MULTIFOCAL HCC

Macroscopic examination of the liver specimens and histological examination confirmed the development of multifocal HCC nodules with a dysmorphic or dyschromic appearance (Fig. 1A) that was markedly attenuated in the animals receiving CeO$_2$NPs. Interestingly, DEN-injured rats treated with CeO$_2$NPs showed a significantly lower liver/body weight ratio (Fig. 1B).

LIVER AND SPLEEN ARE THE MAJOR TARGETS OF CeO$_2$NPs IN HCC RATS

Following intravenous CeO$_2$NPs administration, tissue Ce accumulation was analyzed by ICP-MS. Two weeks after the last administration of CeO$_2$NPs 90.0% and 7.7% of the total dose of Ce collected was located

in the liver and the spleen, respectively, whereas these figures were 77.3% and 21.7% 3 weeks after the completion of the CeO$_2$NPs dosing schedule (Fig. 1C).

SERUM BIOCHEMICAL PARAMETERS AND CIRCULATING LEVELS OF ALPHA-FETOPROTEIN

HCC rats showed significant alterations of liver function tests such as decreased levels of albumin and glucose, higher levels of total bilirubin and total cholesterol, and increased activity of markers of hepatocyte injury such as aspartate aminotransferase, alanine aminotransferase, and gamma-glutamyl transferase. We did not observe significant differences between HCC rats receiving or not receiving CeO$_2$NPs (Supporting Table S2). However, nanoceria administration did significantly reduce the circulating levels of alpha-fetoprotein (AFP), a tumor-associated marker for HCC (Fig. 1B).

EFFECT OF CeO$_2$NPs ON COLLAGEN CONTENT AND CELLULAR APOPTOSIS IN LIVER TISSUE

Long-term administration of DEN promoted incipient formation of fibrotic septa and periportal accumulation of collagen as a consequence of continuous hepatic injury. However, no significant differences in hepatic collagen content were noted between treated and nontreated rats with HCC (Fig. 2A).

The terminal deoxynucleotidyl transferase–mediated deoxyuridine triphosphate nick-end labeling (TUNEL) assay showed a significant increase in positive cells in the liver sections of DEN-injured rats treated with CeO$_2$NPs (Fig. 2B). We also observed a significantly increased protein expression of activated caspase-3 in HCC rats treated with CeO$_2$NPs (Fig. 2C). These results indicate that treatment with CeO$_2$NPs results in acceleration of apoptosis, thereby inhibiting HCC growth.

CeO$_2$NPs DECREASE MACROPHAGE INFILTRATION AND REDUCE INFLAMMATORY GENE OVEREXPRESSION IN LIVER TISSUE

Macrophage infiltration measured by positive cluster of differentiation 68 (CD68) staining was
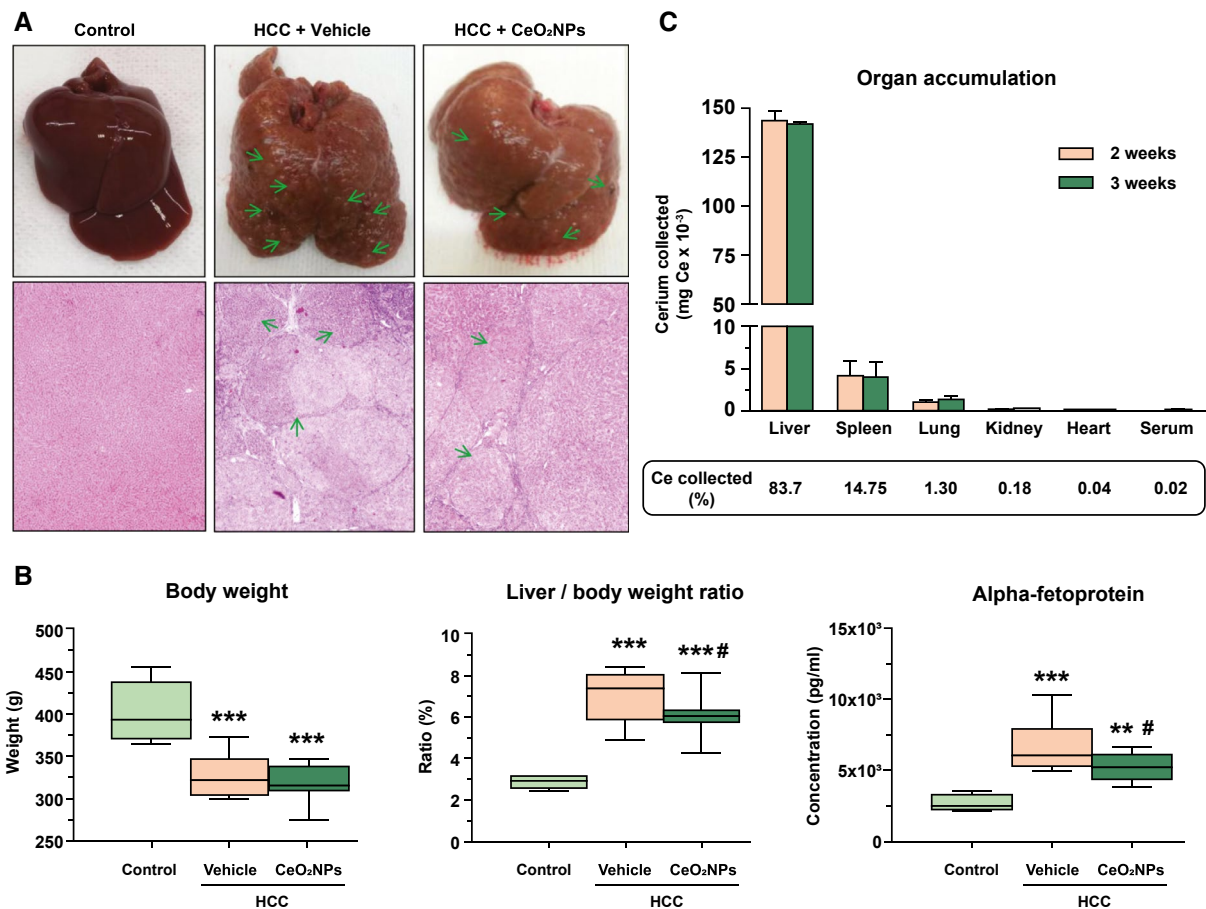
FIG. 1. DEN-induced model of HCC and biodistribution of CeO$_2$NPs. (A) Representative photographs of the liver and hematoxylin and eosin staining (magnification, 40) from control and DEN-injured rats. DEN was administered for 16 weeks, followed by a 2-week washout period. Green arrows point at nodules present in HCC rats. (B) Body weight, liver/body weight ratio, and serum levels of AFP in control rats and HCC rats. Serum samples were collected 1 week after the last dose of CeO$_2$NPs. (C) ICP-MS quantification of cerium. Major organs and serum from HCC rats receiving CeO$_2$NPs collected at two different time points: 2 (n = 3) and 3 (n = 4) weeks after the last administration of CeO$_2$NPs. This corresponds to the nineteenth and twentieth weeks after starting DEN administration. $**P < 0.01$ and $***P < 0.001$ versus control; $^{\#}P < 0.05$ versus HCC + vehicle. One-way analysis of variance and Newman-Keuls *post hoc* test.

observed in intratumoral and peritumoral areas, being significantly lower in HCC rats receiving CeO$_2$NPs (Fig. 3A). mRNA expression of inflammatory, macrophage phenotype, cell growth and differentiation genes was analyzed in liver biopsies of control and HCC rats. Chronic administration of DEN induced higher gene expression of macrophage M1 markers, such as interleukin 1 beta, tumor necrosis factor alpha, inducible nitric oxide synthase, and cyclooxygenase-2 (Supporting Table S3). Interestingly, administration of CeO$_2$NPs significantly down-regulated M1 genes involved in proinflammatory function.

CeO$_2$NPs DECREASE HEPATIC CELLULAR PROLIFERATION

We assessed the effect of CeO$_2$NPs on cell proliferation and the phosphorylation levels of proteins involved in tumor progression. Immunohistochemistry revealed abundant cellular proliferation in liver sections from DEN-injured animals. The cell proliferation rate, measured as the percent of Ki67-positive hepatocyte nuclei, was markedly lower in CeO$_2$NPs-treated rats (Fig. 3B). To ascertain the potential effect of CeO$_2$NPs on interfering with the Ras/mitogen-activated protein kinase (MAPK) signaling pathway,
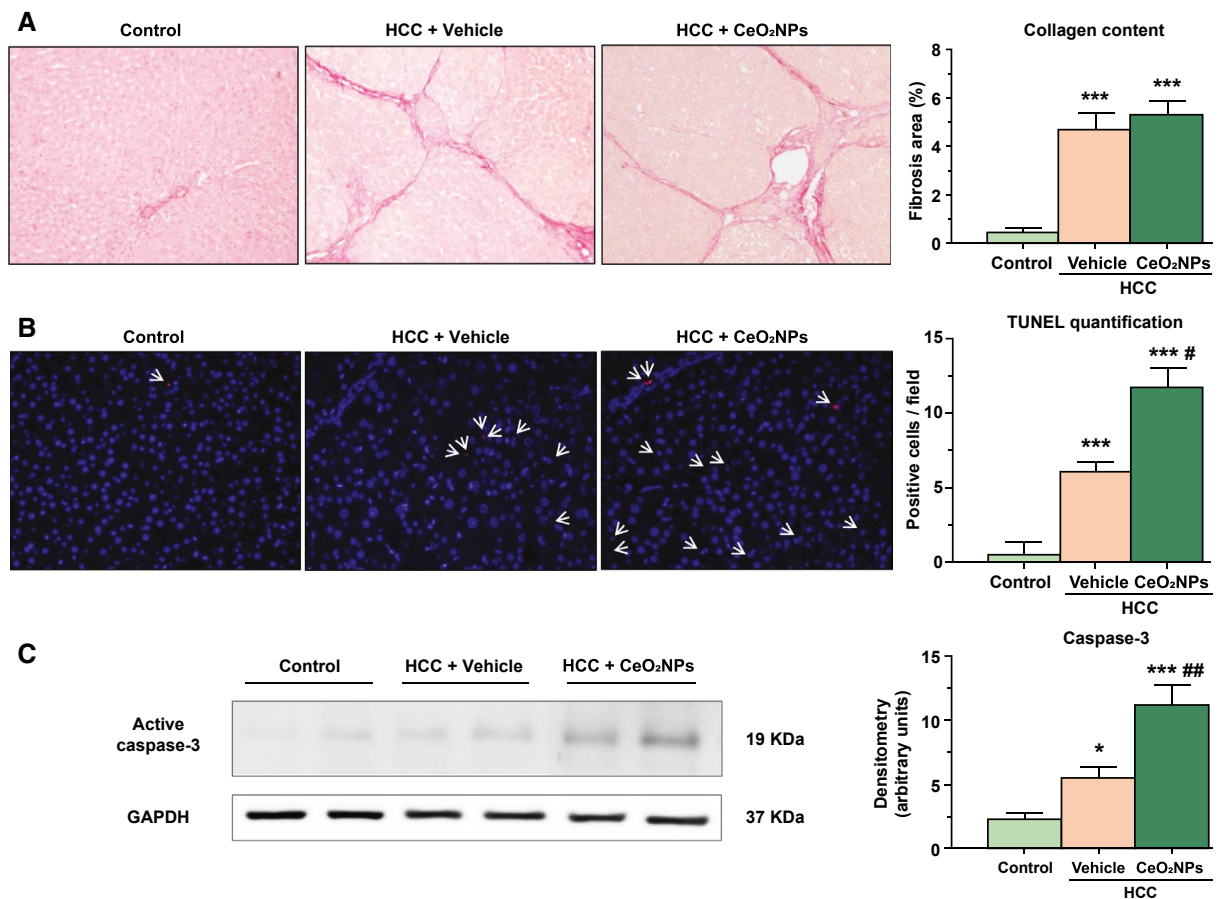
FIG. 2. Effect of CeO_2NPs on hepatic fibrosis and cellular apoptosis. (A) Sirius red staining of representative liver sections obtained from control and DEN–injured rats (magnification, 100). (B) Representative TUNEL assay in liver sections of control rats and HCC rats (magnification, 200). White arrows point to apoptotic (red) cells. (C) Representative western blot for activated caspase-3 in liver tissue of control rats and HCC rats. *$P < 0.05$ and ***$P < 0.001$ versus control group; #$P < 0.05$ and ##$P < 0.01$ versus HCC + vehicle. One-way analysis of variance and Newman-Keuls *post hoc* test, Kruskal-Wallis test, and Dunn's *post hoc* test, with unpaired Student *t* test when appropriate. Abbreviation: GAPDH, glyceraldehyde 3-phosphate dehydrogenase.

we assessed protein expression of total extracellular signal–regulated kinase 1/2 (ERK1/2) and phosphorylated ERK1/2 (P-ERK1/2) in liver samples of HCC rats by western blot. It was of note that CeO_2NPs treatment resulted in a significant reduction of P-ERK1/2 (Fig. 3C). These results suggest that the antiproliferative action of CeO_2NPs is related to interference with the Ras/MAPK signaling pathway in HCC rats.

EFFECT OF CeO_2NPs ON ALTERED CELL SIGNALING PATHWAYS IN LIVER TISSUE

To investigate the effects of CeO_2NPs on kinase-driven signaling pathways, we evaluated the

phosphoproteome profile by mass spectrometry (MS). We identified and quantified a total of 5,048 phosphopeptides in six independent biological replicates that were run twice. Principal component analysis showed that CeO_2NPs-treated samples separate from vehicle-treated samples in principal component 1 (Fig. 4A). At arbitrary threshold values of ±0.8-fold change ($\log_2$) and $P < 0.05$, the phosphorylation of 349 peptides was increased, while the phosphorylation of 133 was decreased after CeO_2NPs treatment (Fig. 4B; Supporting Table S4). This set of regulated phosphopeptides included 20 phosphorylation sites in kinases, of which 11 were increased and nine were decreased (Fig. 4C). Gene ontology analysis showed that cell–cell adhesion and RNA splicing were enriched in the set of genes
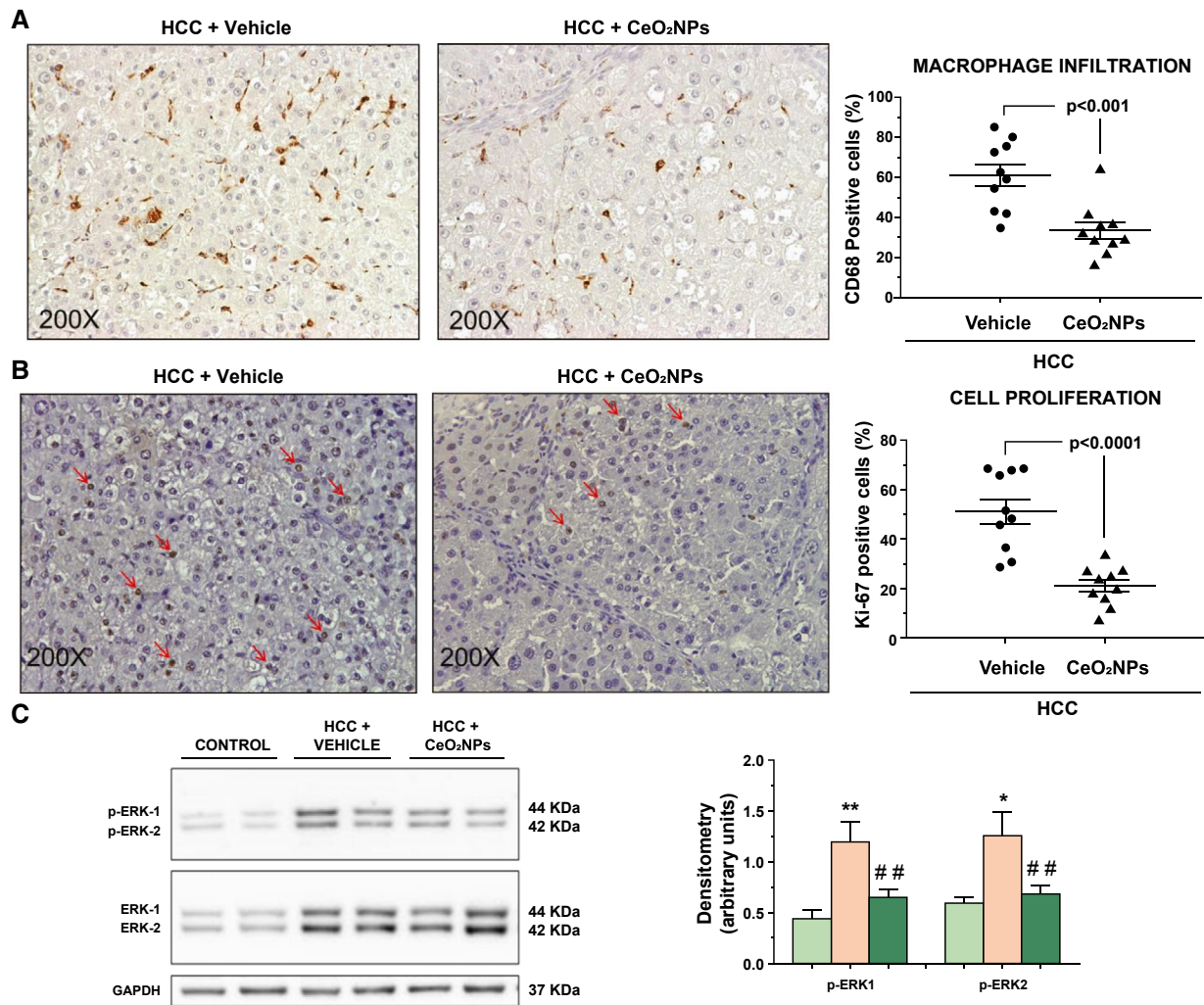
FIG. 3. Effect of CeO$_2$NPs on infiltrating cells, cellular proliferation, and levels of P-ERK1/2 in tumoral tissue. (A) CD68 immunostaining of representative liver sections from HCC rats (magnification, 200). (B) Ki67 immunostaining of representative liver sections from HCC rats (magnification, 200). Red arrows mark nuclei positive for Ki67 staining. (C) Representative western blots of total ERK1/2 and P-ERK1/2 in liver homogenates of control rats and HCC rats. Forty micrograms of protein extracts were loaded per lane. *$P < 0.05$ and **$P < 0.01$ versus control; ##$P < 0.01$ versus HCC + vehicle. One-way analysis of variance and Newman-Keuls *post hoc* test, with unpaired Student t test when appropriate. Abbreviation: GAPDH, glyceraldehyde 3-phosphate dehydrogenase.

that code for the regulated phosphopeptides (Fig. 4D). The set of regulated phosphopeptides linked to cell–cell adhesion included 43 sites in 27 proteins that presented an increased phosphorylation after CeO$_2$NPs treatment and 16 sites in 11 proteins that presented a decreased phosphorylation after NP treatment (Fig. 4E). In addition, proteins linked to cell-matrix adhesion including CD44 and integrin beta 4 (Itgb4) showed a decreased phosphorylation

after CeO$_2$NPs treatment (Fig. 4F). Finally, the set of regulated phosphopeptides linked to RNA splicing included 36 sites in 18 proteins that presented increased phosphorylation and four sites in three proteins that showed decreased phosphorylation (Fig. 4G). These data suggest that CeO$_2$NPs have a global effect on the phosphorylation pattern of liver cells from rats with HCC that mainly affects proteins related to cell adhesion and RNA splicing.
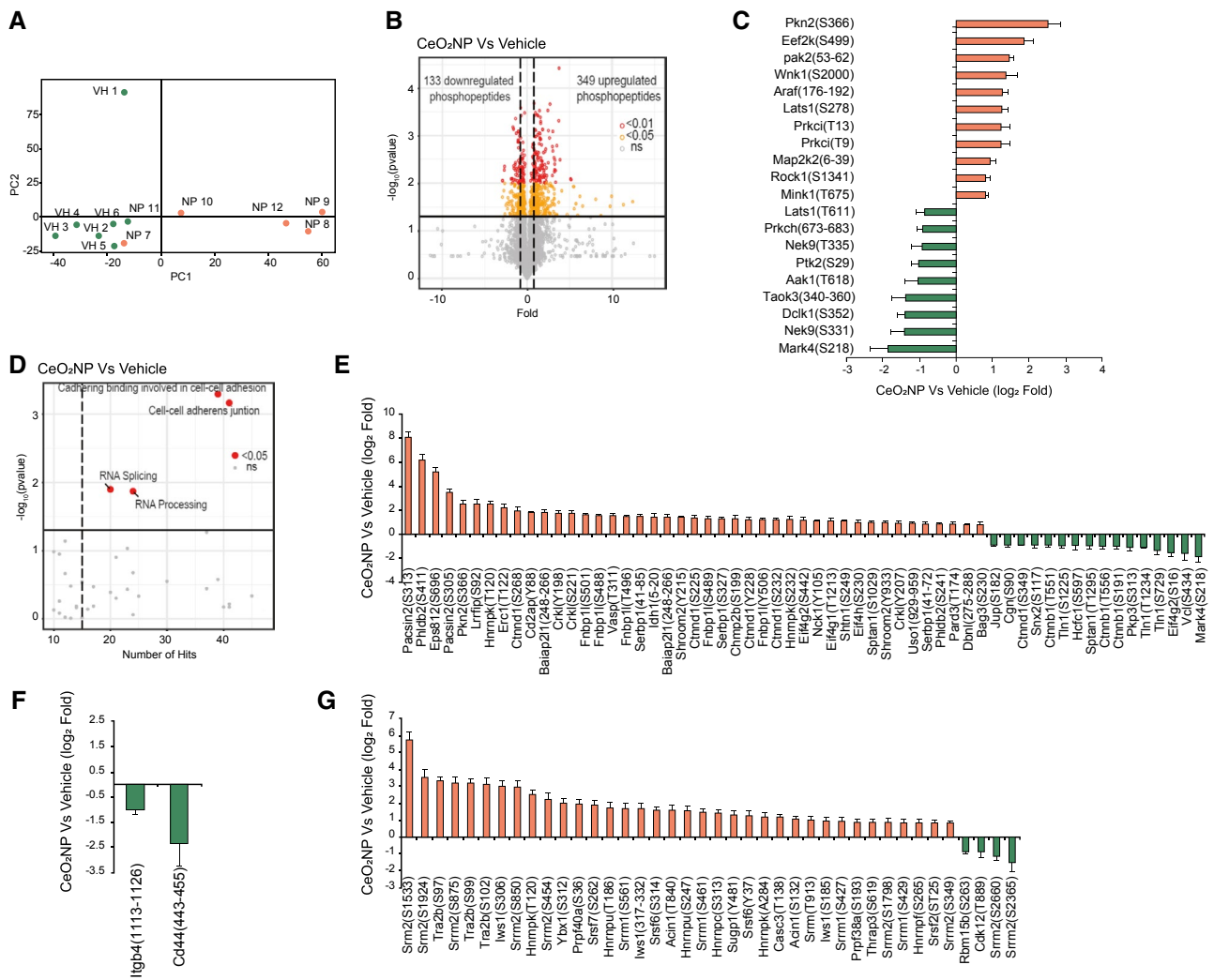
FIG. 4. Effect of CeO$_2$NPs on the phosphoproteome of livers from rats with HCC. (A) Principal component analysis showing the global effect of CeO$_2$NPs on the phosphoproteome of hepatic cells from HCC rats. Blue dots (VH) indicate biological replicates treated with vehicle, while red dots (NP) indicate replicates treated with CeO$_2$NPs. (B) Volcano plot showing phosphopeptides regulated by CeO$_2$NPs. Peptides were considered regulated when $P < 0.05$ (1.3 in $-\log_{10}$ scale) and fold change in $\log_2$ scale >0.8 (increased) or <−0.8 (decreased). Statistical significance was assessed using an unpaired two-tailed Student t test. (C) Chart showing phosphorylation sites in kinases regulated by CeO$_2$NPs treatment. (D) Volcano plot showing gene ontologies enriched in proteins whose phosphorylation was regulated by CeO$_2$NPs. Statistical significance of the enrichment was assessed using a modified Fisher's exact test. (E) Phosphorylation sites linked to cell–cell adhesion and regulated by CeO$_2$NPs treatment. (F) Effect of CeO$_2$NPs treatment over the phosphorylation of CD44 and Itgb4. (G) Phosphorylation sites linked to RNA splicing and regulated by CeO$_2$NPs treatment.

EFFECT OF CeO$_2$NPs ON HEPATIC LIPID METABOLISM

Analysis of total fatty acids (FAs) of principal lipid components in hepatic tissue of HCC animals indicates a dysregulation of FA metabolism mainly occurring in cholesterol ester (CE)– and nonesterified FA (NEFA)– derived FAs (Supporting Table S5). The most important effects induced by CeO$_2$NPs were found in phosphatidylcholine (PC)–derived FAs, which are by far the most abundant lipid component in the liver. In fact, we observed a significant decrease in polyunsaturated FAs (PUFAs), which was exclusively due to a marked diminution in arachidonic acid (AA; C20:4n6; Fig. 5A). We also observed significant changes in C14:0, C16:1, and C17:0, although the differences were quantitatively much less important. Moreover, in NEFA-derived, triglyceride (TG)-derived, and CE-derived FAs, we
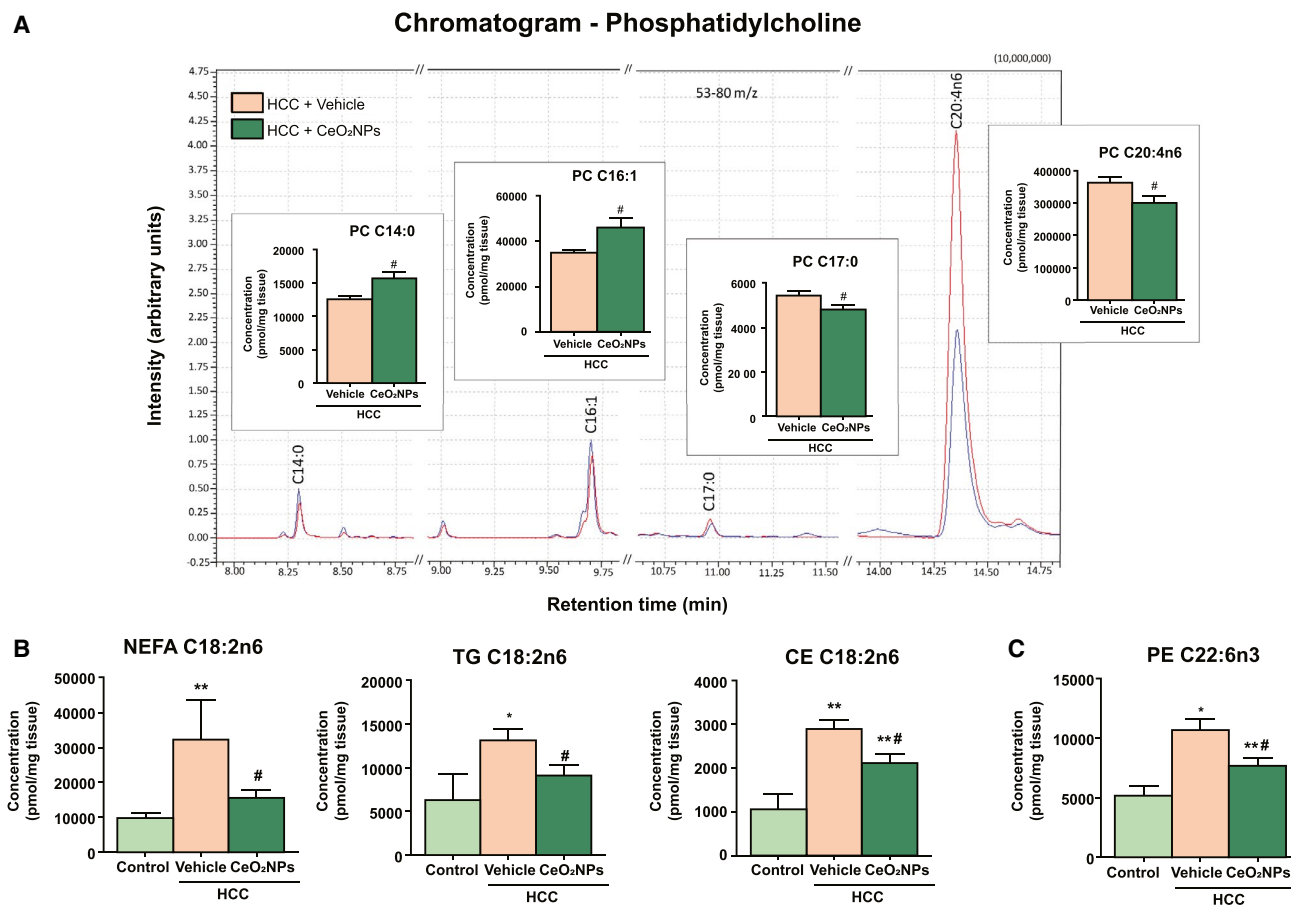
FIG. 5. Representative chromatogram of PC-derived FAs in rats with HCC. (A) Superposition of a representative gas chromatography MS total ion current chromatograms showing the analysis of PC-derived FAs obtained from HCC rats treated with vehicle (red) or CeO$_2$NPs (blue). The represented peaks are the FAs which showed significant differences between groups. Gas chromatography peaks are labeled with the corresponding FA identification. For each peak there is a graph with the quantification of the FA. (B) Effect of nanoceria treatment in linoleic FAs in different lipid components (NEFA, TG, and CE). (C) Effect of CeO$_2$NPs in PE-derived docosahexaenoic acid (C22:6n3). *$P < 0.05$ and **$P < 0.01$ versus control; #$P < 0.05$ versus HCC + vehicle. Unpaired Student t test and Mann-Whitney test when appropriate.

observed that HCC rats showed significantly increased liver content of linoleic acid (LA; C18:2n6) than healthy rats, a phenomenon that was reversed in HCC animals treated with CeO$_2$NPs (Fig. 5B). Of note, on analyzing phosphatidylethanolamine (PE)–derived FAs, we observed that CeO$_2$NPs administration was associated with a significant reduction in the very long chain PUFA docosahexaenoic acid (C22:6n3) (Fig. 5C).

CeO$_2$NPs IMPROVE SURVIVAL IN DEN-INJURED RATS

To assess how the above changes translate into clinical outcome, we investigated the impact of these

NPs on the survival of two groups of HCC rats. The median survival reached by CeO$_2$NPs-treated rats was significantly higher than that in rats receiving vehicle ($P < 0.05$) (Fig. 6A). Next, we were interested in comparing the effect of CeO$_2$NPs to that of sorafenib. Four groups of rats receiving vehicle, CeO$_2$NPs, sorafenib, and CeO$_2$NPs plus sorafenib were investigated. The median survival was markedly lower in HCC rats receiving vehicle (15.5 days, $P < 0.05$) than in those animals receiving CeO$_2$NPs (31 days), sorafenib (33.5 days), or CeO$_2$NPs plus sorafenib (33.5 days) (Fig. 6B). The combined therapy showed the longest survival, although differences did not reach statistical significance.
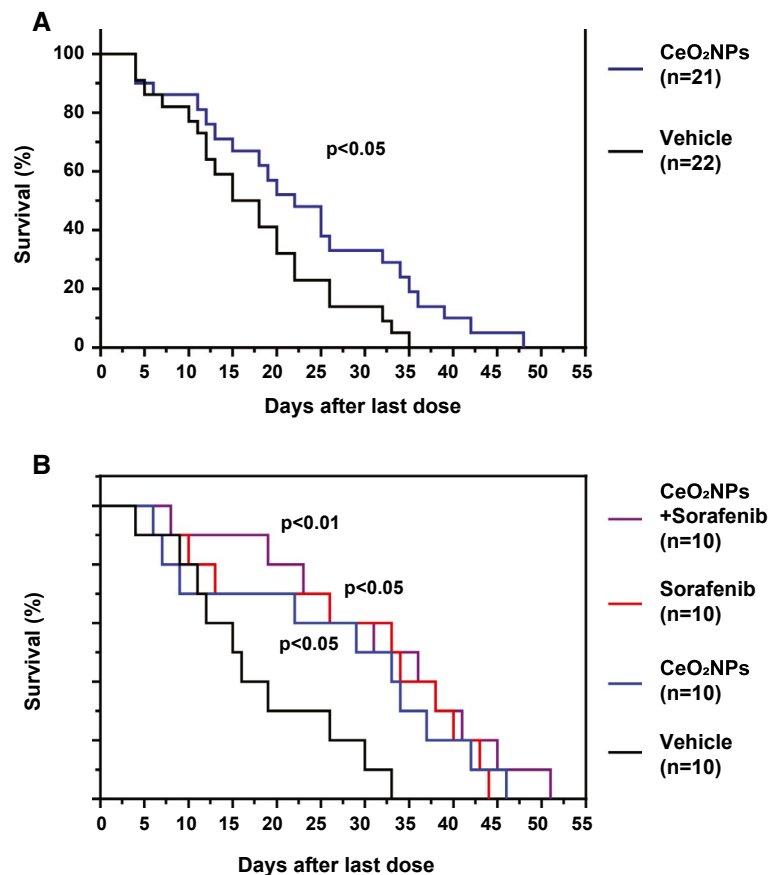
FIG. 6. Effect of CeO_2NPs on survival. (A) HCC rats randomly received two weekly doses of CeO_2NPs or vehicle through the tail vein at the sixteenth and seventeenth weeks, and their survival was analyzed. (B) HCC rats were randomly distributed into four groups receiving vehicle, CeO_2NPs, sorafenib, or the combination CeO_2NPs and sorafenib. Sorafenib was delivered daily by intragastric administration (10 mg/kg) for 14 days. $P < 0.05$ and $P < 0.01$ versus HCC + vehicle, log-rank (Mantel-Cox) test.

CeO_2NPs RETENTION BY HUMAN LIVER

To determine whether CeO_2NPs can be internalized by the human liver, three experimentally viable human livers, declined for transplantation, were perfused with CeO_2NPs under normothermic machine perfusion (NMP) (Supporting Information). Liver function tests and hemodynamic parameters were monitored during perfusion (data not shown) to ensure organ viability and proper device functioning.

To study the cellular uptake and intracellular localization of CeO_2NPs in human livers, ICP-MS and TEM imaging were performed. The concentration of Ce in the serum leaving the liver through the hepatic veins reached the highest levels 15 minutes after NPs administration (Fig. 7A). At 30 minutes of perfusion, the amount of Ce in the perfusate was reduced by at

least 50% when compared to the previous time point and further decreased at 60 minutes. In the case of donor H3, at 60 minutes of NMP, the Ce concentration in the perfusate was still around 45% due to the fact that in this particular organ the injected dose of NPs was almost 100 times higher than in H1 and H2 livers.

Ce subcellular location was examined using conventional bright and enhanced dark field TEM. Liver tissue from all donors was morphologically well preserved, and the cells presented a viable morphology. Liver biopsies obtained from donor H3 were examined under conventional TEM and energy-dispersive X-ray spectroscopy (EDX). In conventional TEM, CeO_2NPs appeared as small, dense, black structures in the form of agglomerates of different sizes inside blood vessels, the space of Disse, endothelial cells, and some blood circulating cells (Fig. 7B). CeO_2NPs
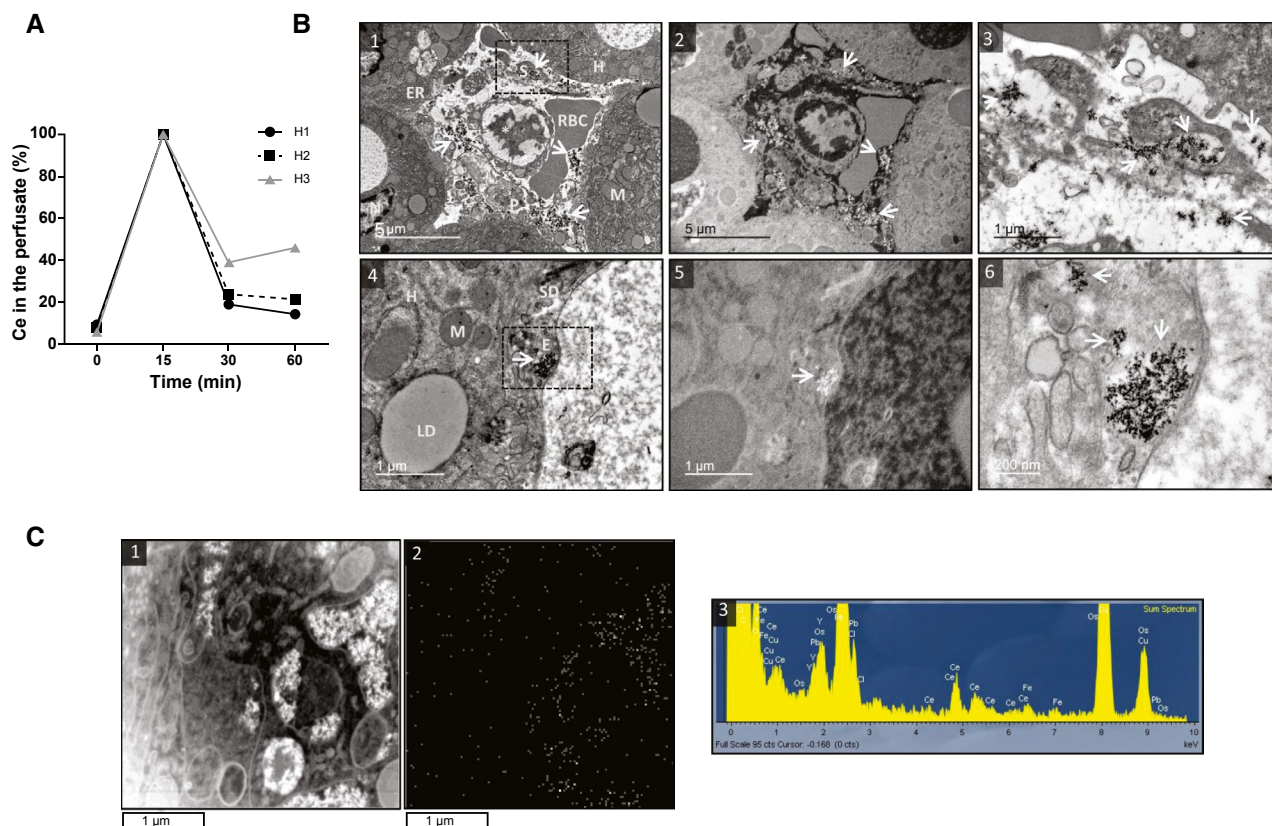
FIG. 7. Accumulation of Ce in isolated human livers. (A) Amount of Ce in the perfusate 0, 15, 30, and 60 minutes after NP administration. ICP-MS data are expressed as percent of Ce present in the perfusate compared to the highest Ce amount present in the serum of each liver. (B) Assessment of CeO_2NPs subcellular location in human hepatic tissue after 1 hour of NP infusion; (1,2,3) TEM image of a blood vessel containing NPs surrounded by hepatocytes. In bright field (1), aggregates of CeO_2NPs (white arrows) appear as dark, electrodense spots. In dark field (2), nanoparticles are seen bright. (3) Magnified view of the boxed area depicting the nanoparticles in the space of Disse. (4,5) TEM image of a hepatocyte in the proximity of an endothelial cell containing CeO_2NPs, bright and dark field, respectively. (6) High-magnification micrograph of the boxed area showing in detail the NPs inside the endothelial cell. *Apoptotic cell. (C) (1) STEM-HAADF image of endosome-like vesicles of an endothelial cell. (2) STEM-EDX element-distribution map showing the spatial distribution of Ce in the region outlined. Four adjacent pixel/spectra binned for each point. (3) EDX sum spectrum (Y = counts, X = keV) showing the average elemental composition of the image. Abbreviations: E, endothelial cell; ER, endoplasmic reticulum; H, hepatocyte; LD, lipid droplet; M, mitochondria; N, nucleus; P, platelet; RBC, red blood cell; S, sinusoid; SD, space of Disse.

were observed both free and within intracellular, single-membrane, endosome-like organelles. In dark field TEM, given its high atomic number relative to the elements typically found in organic tissues, Ce is expected to appear as very bright dots, as shown in Fig. 7B. The presence of Ce was further confirmed using high-angle annular dark-field scanning transmission electron microscopy (HAADF-STEM), which provides structural and chemical information with atomic resolution. Figure 7C shows a representative region in the set of analyzed images. The elemental map (central panel) shows the spatial distribution of Ce in the region outlined in the left panel, and the

EDX spectrum (right panel) confirms the elemental composition. In addition to Os from the postfixation, Cu from the TEM grid, and Pb from the staining, Ce is the only element detected by using EDX analysis.

CeO_2NPs ADSORPTION BY HUMAN HEPATOCYTE CANCER CELLS

To assess whether human hepatocytes can internalize CeO_2NPs, HepG2 cells, a human derived cell cancer line, were exposed to CeO_2NPs (10 μg/mL) for 24 hours and subjected to TEM analysis. NPs were
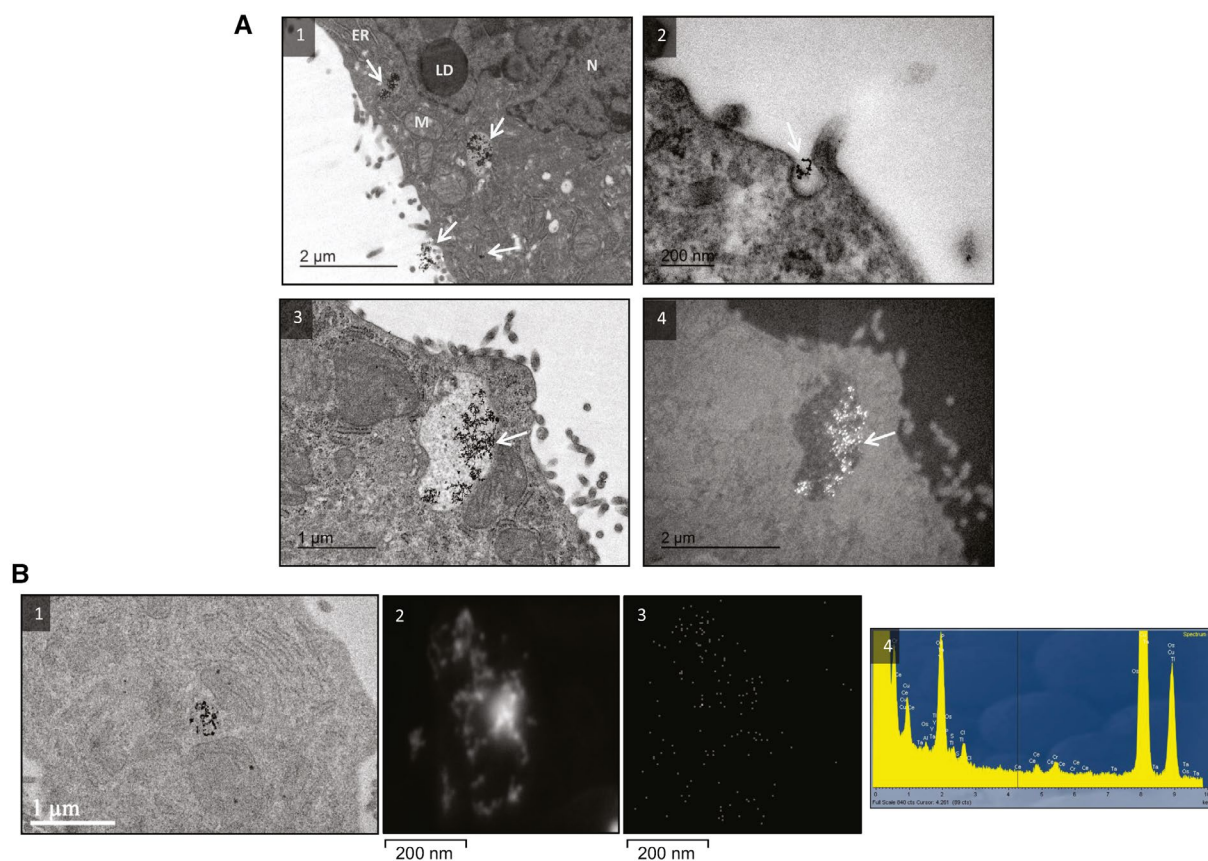
1277

FIG. 8. CeO$_2$NPs adsorption in human hepatocyte cancer cells. (A) TEMs of HepG2 cells showing the uptake of NPs: (1) hepatocyte exposed to CeO$_2$NPs (white arrows) for 24 hours, with some NPs adhering to the cell membrane, others confined to vesicles, and a few free in the cytoplasm; (2) formation of pseudopodia with NPs in the center; (3,4) vesicle loaded with CeO$_2$NPs in bright and dark fields, respectively. (B) (1) TEM image displaying NPs in the cytoplasm of a hepatocyte; (2) STEM-HAADF image from the NPs; (3) Ce elemental mapping with four adjacent pixel/spectra binned for each point; (4) EDX sum spectrum (Y = counts, X = keV) showing the average elemental composition of the image. Abbreviations: ER, endoplasmic reticulum; LD, lipid droplet; M, mitochondria; N, nucleus.

strongly attached to the outer leaflet of the plasmatic membrane, free in the cytoplasm, and mostly inside numerous endosome-like bodies of diverse morphology (Fig. 8A). The mitochondria, the endoplasmic reticulum, and the nucleus of these hepatocytes appeared normal. To verify that the electron-dense granules were indeed CeO$_2$NPs, we performed dark field microscopy followed by HAADF-STEM. In both dark field TEM and STEM, NPs appeared as bright spots. The Ce elemental map and EDX spectrum confirmed the presence of Ce in the preparations (Fig. 8B).

Discussion

The ability of nanoceria to catalyze redox reactions has been widely used in petrochemical industries and catalytic exhaust converters for decades.[33] The use of these NPs as a therapeutic tool is still a matter of concern. This is mainly due to the tendency of CeO$_2$NPs to evolve when in contact with physiological media.[34] Variability in the response and loss of antioxidant activity are the outcomes of these alterations. In the current investigation, some of these difficulties have been overcome by preparing albumin-coated CeO$_2$NPs with high monodispersity and high stability in the physiological media. This coating prevents the development of large NP aggregates and protein corona formation, resulting in a stable colloidal solution with sustained and more intense effects.

Unfortunately, HCC is still rather orphan in terms of highly effective systemic treatment. In this context, oxidative stress, mainly contributed by ROS, has

been implicated in the pathogenesis of several diseases including cancer. It is well known that ROS can drive the initial development and progression of cancer as well as down-regulate antioxidant enzymes that normally combat free radical production.[10] Consequently, many antioxidant compounds, enzymes, and inhibitors of reduced nicotinamide adenine dinucleotide phosphate oxidase have been studied for treating chronic inflammation and cancer. However, results to date have been suboptimal, mainly due to their low systemic bioavailability and insufficient levels at the target sites.

Here we consider that CeO_2NPs could be an NP-based therapy platform in HCC, which would be able to induce ROS degradation and tumor recession by virtue of their great self-regenerating antioxidant capacity. Because the antioxidant effect of CeO_2NPs is catalytic and consequently permanent, this would represent a clear competitive advantage over other antioxidant therapies needing permanent application. In addition, CeO_2NPs are only active as a catalyst when there is an excess of ROS; otherwise, they are inert and appear innocuous.

The carcinogenic effect of DEN is due to an enhancement of hepatocyte proliferation mainly in the centrilobular hepatocytes. DEN is bioactivated following hydroxylation by the cytochrome P450 (CYP) system; then, the hydroxylated DEN is oxidized by CYP2E1 to reactive products in rat liver liposomes. DEN-treated rats displayed macroscopically distorted liver, with altered liver weight and anomalous microscopic architecture of the liver parenchyma showing diffuse dysplasia and fibrotic tracts. This prompted us to assess whether the HCC liver, as indeed occurs in the normal liver, is also a main target for CeO_2NPs. Our results further confirm that, even in a liver with intense tumorigenic activity, CeO_2NPs maintain their high selective targeting on the hepatic tissue.

Parameters indicating altered tissue growth or proliferation and ongoing proinflammatory processes were significantly less activated in rats receiving CeO_2NPs. Treated rats showed increased liver/body weight ratio, decreased macrophage infiltration, and lower amount of Ki67-positive cells. Ki67 is a nuclear antigen extensively used as a proliferation marker and as a prognostic indicator for cancer. We also observed decreased serum concentration of AFP, the main serological biomarker of dedifferentiation

of hepatocytes that is associated with the development of HCC. This occurred in the frame of attenuated macrophage M1 proinflammatory gene expression in the liver tissue of HCC-treated rats. Tumor-associated macrophages are well known for their trophic abilities and for providing immunosuppressive tumor microenvironment and therefore facilitating tumor progression.[35] In that sense, lowering macrophage numbers in liver tissue by means of chemotaxis inhibition or cell death could partially explain the antitumor effects of nanoceria.

Evidence supports that CeO_2NPs have a specific antitumorigenic effect in HCC rats. First, following NPs administration, we observed increased liver apoptotic activity. This is consistent with previous studies describing that after exposure to antioxidant cuprous oxide NPs, lung melanoma cells activate caspase-3 and caspase-9, inducing apoptosis of tumor cells.[36] On the other hand, CeO_2NPs also resulted in decreased levels of P-ERK1/2, an essential component of the Ras/Raf/MAPK kinase/ERK signaling pathway. This is among the principal routes controlling cell survival, differentiation, proliferation, growth, angiogenesis, regulation of glucose and lipid metabolism, and inflammation.[37]

The impact of CeO_2NPs on cell phosphorylation in HCC has not been systematically investigated using untargeted MS-based proteomics. Our initial principal component analysis suggests a global effect of CeO_2NPs over protein phosphorylation in the liver of HCC rats that significantly affected 9.5% of all detected phosphorylation sites. The effect of CeO_2NPs comprised both increased and decreased phosphorylation. The administration of CeO_2NPs affected kinases involved in signaling pathways related to apoptosis, cell proliferation, migration, and survival such as p21 (RAC1) activated kinase 2, eukaryotic elongation factor 2 kinase, protein tyrosine kinase 2/focal adhesion kinase 2, and NIMA-related kinase 9. Interestingly, a gene ontology analysis showed an enrichment of proteins linked to RNA splicing and cell–cell adhesion in the subset of proteins whose phosphorylation were significantly regulated after CeO_2NPs treatment. Splicing is a process frequently deregulated in cancer cells because it can regulate the function of key proteins involved in apoptosis, proliferation, angiogenesis, and migration.[38] In this regard, CeO_2NPs treatment that reduced cell proliferation caused both an increase and a decrease in the phosphorylation of proteins involved in splicing. Cell adhesion is also a

process heavily deregulated in cancer cells with multiple proteins involved in cell–cell adhesion considered as tumor suppression or oncogenes.[39] Our gene ontology analysis indicates that CeO$_2$NPs produce a large effect on the phosphorylation pattern of proteins involved in cell–cell adhesion with proteins presenting both overphosphorylation and downphosphorylation, suggesting an alteration in this biological process. We observed a reduced phosphorylation of two other cell surface proteins involved in cell adhesion, CD44 and Itgb4.

A hallmark of cancer cells is dysregulation of FA metabolism to support proliferation.[40] Accordingly, total serum TG and cholesterol were found to be significantly decreased in HCC rats. Highly proliferative cancer cells have strong lipid and cholesterol avidity; consequently, these cells either increase the uptake of exogenous lipids or overactivate their endogenous synthesis.[41] Excessive lipids and cholesterol in cancer cells are stored in lipid droplets as cholesteryl esters,[37] which is in agreement with our findings of increased CE-derived FAs in hepatic HCC tissue. The analysis of principal lipid components also revealed an increase in NEFA probably due to an increased generation to support tumor growth.

The most important effects induced by CeO$_2$NPs are found in PC-derived FAs. The decrease in PC-PUFAs resulting from CeO$_2$NPs administration was mostly due to a decrease in AA.[42] Phospholipases A2, C, and D can mediate the release of esterified AA from cellular phospholipids, a process which already seems incremented in HCC. Free AA can be metabolized through enzymatic reactions or act as a second messenger in signal transduction pathways[43]; some of these pathways were demonstrated to be significantly up-regulated in our HCC rats. After nanoceria treatment, the decrease in esterified PC-AA was more pronounced. This phenomenon seems to be related to the increase of apoptosis in these rats because free AA is able to promote the activation of sphingomyelinase and the apoptotic process.[44]

CeO$_2$NPs treatment reversed the increase in NEFA-derived, TG-derived, and CE-derived LA in HCC rats. LA, one of the most abundant FAs in all lipid components, has been reported to change the metabolism of intrahepatic CD4$^+$ T cells, leading them to apoptosis and, thus, contributing to HCC development.[44] Neoplastic hepatocyte lesions have been associated with changes in the PUFA profile,

which are likely due to an abnormal essential FA metabolism involving Δ-6 desaturase (Δ-6D).[43] The activity and expression of this desaturase are regulated by the intracellular redox state.[45] This suggests that the restoration of normal hepatic levels of LA in the HCC rats treated with CeO$_2$NPs could result from the reactivation of Δ-6D activity due to the reduction in oxidative stress.

The translation of the antitumorigenic effects induced by CeO$_2$NPs into a clinically significant improvement was assessed by investigating the effect of CeO$_2$NPs on survival. Treated HCC rats showed a clear amelioration in this parameter. To date, tyrosine kinase inhibitors, such as sorafenib, lenvatinib, cabozatinib, or regorafenib, as well as the antiangiogenic antibody ramucirumab, are considered effective therapies in patients with advanced HCC.[46] The effect of CeO$_2$NPs on overall survival was similar to that observed with sorafenib, which indicates that these NPs are at least as effective as sorafenib under the conditions studied. The combination of both treatments did not result in an additional improvement in survival in comparison to each treatment administered alone. CeO$_2$NPs and sorafenib likely interfere with common signaling pathways, such as angiogenesis through vascular endothelial growth factor signaling, which would explain why the combination of both compounds did not result in any additional effect. The effects of CeO$_2$NPs on the ERK1/2 signaling pathway, the modulation of the phosphorylation state of a high number of peptides, and their manifestations on cell proliferation and apoptosis mirror some the abundant data reported on sorafenib effects.[47]

For a comprehensive understanding of whether the behavior of CeO$_2$NPs in the human liver resembles that observed in rats with HCC, we administered nanoceria to human livers under *ex vivo* normothermic perfusion. The *ex vivo* experiments confirmed that CeO$_2$NPs have high avidity for human liver because they accumulate in the target tissue readily after administration. The NPs were found both free and within intracellular, single-membrane, endosome-like organelles. The elemental analysis combined with the STEM helped us to confirm their presence and distinguish them from endogenous structures and artifacts in the tissue. Moreover, *in vitro* experiments with the HepG2 cell line confirmed the uptake and retention of

CeO$_2$NPs by human hepatocyte cancer cells mostly in endosome-like bodies.

In conclusion, these results indicate that the antioxidant properties of CeO$_2$NPs partially revert cell mechanisms involved in tumor progression and significantly increase survival in HCC rats, indicating that this inorganic nanomaterial represents an effective treatment in experimental HCC. These findings suggest that CeO$_2$NPs alone or in combination with the current molecular targeted therapies could be effective at stopping or attenuating the tumoral progression in patients with HCC.

REFERENCES

1) Bray F, Ferlay J, Soerjomataram I, Siegel R, Torre L, Jemal A. Global cancer statistics 2018: GLOBOCAN estimates of incidence and mortality worldwide for 36 cancers in 185 countries. CA Cancer J Clin 2018;68:394-424.

2) European Association for the Study of the Liver. EASL clinical practice guidelines: management of hepatocellular carcinoma. J Hepatol 2018;69:182-236.

3) Zhang DY, Friedman SL. Fibrosis-dependent mechanisms of hepatocarcinogenesis. HEPATOLOGY 2012;56:769-775.

4) Guichard C, Amaddeo G, Imbeaud S, Ladeiro Y, Pelletier L, Maad IB, et al. Integrated analysis of somatic mutations and focal copy-number changes identifies key genes and pathways in hepatocellular carcinoma. Nat Genet 2012;44:694-698.

5) Llovet JM, Ricci S, Mazzaferro V, Hilgard P, Gane E, Blanc JF, et al. Investigators study group. Sorafenib in advanced hepatocellular carcinoma. N Engl J Med 2008;359:378-390.

6) Cheng AL, Kang YK, Chen Z, Tsao CJ, Qin S, Kim JS, et al. Efficacy and safety of sorafenib in patients in the Asia-Pacific region with advanced hepatocellular carcinoma: a phase III randomised, double-blind, placebo-controlled trial. Lancet Oncol 2009;10:25-34.

7) van Malenstein H, Dekervel J, Verslype C, Van Cutsem E, Windmolders P, Nevens F, et al. Long-term exposure to sorafenib of liver cancer cells induces resistance with epithelial-to-mesenchymal transition, increased invasion and risk of rebound growth. Cancer Lett 2013;329:74-83.

8) Bruix J, Qin S, Merle P, Granito A, Huang YH, Bodoky G, et al.; RESORCE Investigators. Regorafenib for patients with hepatocellular carcinoma who progressed on sorafenib treatment (RESORCE): a randomised, double-blind, placebo-controlled, phase 3 trial. Lancet 2017;389:56-66.

9) Forner A, Reig M, Bruix J. Hepatocellular carcinoma. Lancet 2018;391:1301-1314.

10) Waris G, Ahsan H. Reactive oxygen species: role in the development of cancer and various chronic conditions. J Carcinog 2006;5:14.

11) **Calvisi DF**, **Conner EA**, Ladu S, Lemmer ER, Factor VM, Thorgeirsson SS. Activation of the canonical Wnt/beta-catenin pathway confers growth advantages in c-Myc/E2F1 transgenic mouse model of liver cancer. J Hepatol 2005;42:842-849.

12) Roskams T, Yang SQ, Koteish A, Durnez A, DeVos R, Huang X, et al. Oxidative stress and oval cell accumulation in mice and humans with alcoholic and nonalcoholic fatty liver disease. Am J Pathol 2003;163:1301-1311.

13) Laviña B, Gracia-Sancho J, Rodríguez-Vilarrupla A, Chu Y, Heistad DD, Bosch J, et al. Superoxide dismutase gene transfer reduces portal pressure in CCl$_4$ cirrhotic rats with portal hypertension. Gut 2009;58:118-125.

14) Heckert EG, Karakoti AS, Seal S, Self WT. The role of cerium redox state in the SOD mimetic activity of nanoceria. Biomaterials 2008;29:2705-2709.

15) Pirmohamed T, Dowding JM, Singh S, Wasserman B, Heckert E, Karakoti AS, et al. Nanoceria exhibit redox state-dependent catalase mimetic activity. Chem Commun (Camb) 2010;46:2736-2738.

16) Cafun JD, Kvashnina KO, Casals E, Puntes VF, Glatzel P. Absence of Ce3+ sites in chemically active colloidal ceria nanoparticles. ACS Nano 2013;7:10726-10732.

17) Heckert EG, Seal S, Self WT. Fenton-like reaction catalyzed by the rare earth inner transition metal cerium. Environ Sci Technol 2008;42:5014-5019.

18) Chen J, Patil S, Seal S, McGinnis JF. Rare earth nanoparticles prevent retinal degeneration induced by intracellular peroxides. Nat Nanotechnol 2006;1:142-150.

19) Schubert D, Dargusch R, Raitano J, Chan SW. Cerium and yttrium oxide nanoparticles are neuroprotective. Biochem Biophys Res Commun 2006;342:86-91.

20) Pourkhalili N, Hosseini A, Nili-Ahmadabadi A, Hassani S, Pakzad M, Baeeri M, et al. Biochemical and cellular evidence of the benefit of a combination of cerium oxide nanoparticles and selenium to diabetic rats. World J Diabetes 2011;2:204-210.

21) Kim CK, Kim T, Choi IY, Soh M, Kim D, Kim YJ, et al. Ceria nanoparticles that can protect against ischemic stroke. Angew Chem Int Ed Engl 2012;51:11039-11043.

22) Niu J, Azfer A, Rogers LM, Wang X, Kolattukudy PE. Cardioprotective effects of cerium oxide nanoparticles in a transgenic murine model of cardiomyopathy. Cardiovasc Res 2007;73:549-559.

23) Colon J, Hsieh N, Ferguson A, Kupelian P, Seal S, Jenkins DW, et al. Cerium oxide nanoparticles protect gastrointestinal epithelium from radiation-induced damage by reduction of reactive oxygen species and upregulation of superoxide dismutase 2. Nanomedicine 2010;6:698-705.

24) Li H, Liu C, Zeng YP, Hao YH, Huang JW, Yang ZY, et al. Nanoceria-mediated drug delivery for targeted photodynamic therapy on drug-resistant breast cancer. ACS Appl Mater Interfaces 2016;8:31510-31523.

25) Nourmohammadi E, Khoshdel-Sarkarizi H, Nedaeinia R, Sadeghnia HR, Hasanzadeh L, Darroudi M, et al. Evaluation of anticancer effects of cerium oxide nanoparticles on mouse fibrosarcoma cell line. J Cell Physiol 2019;234:4987-4996.

26) Tarnuzzer RW, Colon J, Patil S, Seal S. Vacancy engineered ceria nanostructures for protection from radiation-induced cellular damage. Nano Lett 2005;5:2573-2577.

27) Patel P, Kansara K, Singh R, Shukla RK, Singh S, Dhawan A, et al. Cellular internalization and antioxidant activity of cerium oxide nanoparticles in human monocytic leukemia cells. Int J Nanomed 2018;13:39-41.

28) Oró D, Yudina T, Fernández-Varo G, Casals E, Reichenbach V, Casals G, et al. Cerium oxide nanoparticles reduce steatosis, portal hypertension and display anti-inflammatory properties in rats with liver fibrosis. J Hepatol 2016;64:691-698.

29) Adebayo OA, Akinloye O, Adaramoye OA. Cerium oxide nanoparticles attenuate oxidative stress and inflammation in the liver of diethylnitrosamine-treated mice. Biol Trace Elem Res 2020;193:214-225.

30) Córdoba-Jover B, Arce-Cerezo A, Ribera J, Pauta M, Oró D, Casals G, et al. Cerium oxide nanoparticles improve liver regeneration after acetaminophen-induced liver injury and partial hepatectomy in rats. J Nanobiotechnology 2019;17:112.

31) Carvajal S, Perramón M, Oró D, Casals E, Fernández-Varo G, Casals G, et al. Cerium oxide nanoparticles display antilipogenic effect in rats with non-alcoholic fatty liver disease. Sci Rep 2019;9:12848.

32) Casals E, Gusta MF, Piella J, Casals G, Jiménez W, Puntes V. Intrinsic and extrinsic properties affecting innate immune responses to nanoparticles: the case of cerium oxide. Front Immunol 2017;8:970.

33) Reed K, Cormack A, Kulkarni A, Mayton M, Sayle D, Klaessigf F, et al. Exploring the properties and applications of nanoceria: is there still plenty of room at the bottom? Environ Sci Nano 2014;1:390-405.

34) Casals E, Gonzalez E, Puntes VF. Reactivity of inorganic nanoparticles in biological environments: insights into nanotoxicity mechanisms. J Phys D Appl Phys 2012;45:44.

35) Krenkel O, Tacke F. Liver macrophages in tissue homeostasis and disease. Nat Rev Immunol 2017;17:306-321.

36) Wang Y, Yang F, Zhang HX, Zi XY, Pan XH, Chen F, et al. Cuprous oxide nanoparticles inhibit the growth and metastasis of melanoma by targeting mitochondria. Cell Death Dis 2013;29:e783.

37) Asati V, Mahapatra DK, Bharti SK. PI3K/Akt/mTOR and Ras/Raf/MEK/ERK signaling pathways inhibitors as anticancer agents: structural and pharmacological perspectives. Eur J Med Chem 2016;109:314-341.

38) Czubaty A, Piekiełko-Witkowska A. Protein kinases that phosphorylate splicing factors: roles in cancer development, progression and possible therapeutic options. Int J Biochem Cell Biol 2017;91:102-115.

39) Fearnley GW, Young KA, Edgar JR, Antrobus R, Hay IM, Liang WC, et al. The homophilic receptor PTPRK selectively dephosphorylates multiple junctional regulators to promote cell–cell adhesion. eLife 2019;8:e44597.

40) Röhrig F, Schulze A. The multifaceted roles of fatty acid synthesis in cancer. Nat Rev Cancer 2016;16:732-749.

41) Bechmann LP, Hannivoort RA, Gerken G, Hotamisligil GS, Trauner M, Canbay A. The interaction of hepatic lipid and glucose metabolism in liver diseases. J Hepatol 2012;56:952-964.

42) Hanna VS, Hafez EAA. Synopsis of arachidonic acid metabolism: a review. J Adv Res 2018;11:23-32.

43) Abel S, Smuts CM, de Villiers C, Gelderblom WC. Changes in essential fatty acid patterns associated with normal liver regeneration and the progression of hepatocyte nodules in rat hepatocarcinogenesis. Carcinogenesis 2001;22:795-804.

44) Brown ZJ, Fu Q, Ma C, Kruhlak M, Zhang H, Luo J, et al. Carnitine palmitoyltransferase gene upregulation by linoleic acid induces CD4^{+} T cell apoptosis promoting HCC development. Cell Death Dis 2018;9:620.

45) Valenzuela R, Echeverria F, Ortiz M, Rincón-Cervera MÁ, Espinosa A, Hernandez-Rodas MC, et al. Hydroxytyrosol prevents reduction in liver activity of Δ-5 and Δ-6 desaturases, oxidative stress, and depletion in long chain polyunsaturated fatty acid content in different tissues of high-fat diet fed mice. Lipids Health Dis 2017;16:64.

46) Bruix J, Reig M, Sherman M. Evidence-based diagnosis, staging, and treatment of patients with hepatocellular carcinoma. Gastroenterology 2016;150:835-853.

47) Wilhelm SM, Adnane L, Newell P, Villanueva A, Llovet JM, Lynch M. Preclinical overview of sorafenib, a multikinase inhibitor that targets both Raf and VEGF and PDGF receptor tyrosine kinase signaling. Mol Cancer Ther 2008;7:3129-3140.

Author names in bold designate shared co-first authorship.

Supporting Information

Additional Supporting Information may be found at onlinelibrary.wiley.com/doi/10.1002/hep.31139/suppinfo.